Effects of nano HAP on biological and structural properties of glass bone cement

Qiang Fu,[1] Nai Zhou,[1] Wenhai Huang,[1] Deping Wang,[1] Liying Zhang,[1] Haifeng Li[2]
[1]*School of Materials Science and Engineering, Tongji University, Shanghai, 200092, PR China*
[2]*Tongji Hospital Affiliated Tongji University, Shanghai, 200065, PR China*

Received 28 April 2004; revised 29 August 2004; accepted 30 August 2004
Published online 16 June 2005 in Wiley InterScience (www.interscience.wiley.com). DOI: 10.1002/jbm.a.30322

Abstract: A novel type of glass-based nanoscale hydroxyapatite (HAP) bioactive bone cement (designed as GBNHAPC) was synthesized by adding nanoscale hydroxyapatite crystalline (20–40 nm), into the self-setting glass-based bone cement (GBC). The inhibition rate of nanoscale HAP and micron HAP on osteosarcoma U2-OS cells was examined. The effects of nanoscale HAP on the crystal phase, microstructure and compressive strength of GBNHAPC were studied, respectively. It was concluded that nanoscale HAP could inhibit the cell proliferation, whereas micron HAP could not, and that nanoscale HAP could be dispersed in the cement evenly and the morphology did not change significantly after a longer immersion time. XRD and FTIR results show nanoscale HAP did not affect the setting reaction of the cement. Furthermore, GBNHAPC had a higher compressive strength (92.6 ± 3.8 MPa) than GBC (80.1 ± 3.0 MPa). It was believed that GBNHAPC might be a desirable biomaterial that could not only fill bone defects but also inhibit cancer cell growth. © 2005 Wiley Periodicals, Inc. J Biomed Mater Res 74A: 156–163, 2005

Key words: nanoscale hydroxyapatite; bone cement; cell proliferation

INTRODUCTION

Bone cement, as a desirable repairing material for bone defects, has attracted great attention in biomedical field. Polymethyl methacrylate (PMMA), traditional bone cement, has recently been replaced by inorganic bone cement because of its potential harmfulness of degraded products to human body.[1] Calcium phosphate cement (CPC) and glass based bone cement (GBC) have aroused great interest in bone defects repairing field, because of their excellent biocompatibility and high mechanical strength. Because the mechanical strength of CPC is lower than that of GBC, most researches are recently concentrated on the synthesis of bioactive glass powder with such resins as BIS-GMA and PMMA to get an even higher mechanical strength.[2,3] However, little attention is attracted to the method of enhancing the mechanical strength by introducing inorganic biomaterials into GBC. Latest research[4] shows that a smaller size of hydroxyapatite (HAP, $Ca_{10}(PO_4)_6(OH)_2$) will result in a higher mechanical strength and that nano HAP crystallite could inhibit the growth of certain kinds of cancer cells, such as liver and throat cancer cells, while having few side effects on normal cells.[5,6] This makes it possible that nano HAP might be used as an anticancer material. However, the mechanical strength of HAP crystallite alone is so low that it can not form a fixed shape in human body, which hinders the clinical application of nanoscale HAP crystallite in bone defects repairing.

In this article, nano HAP was introduced into GBC to produce a novel inorganic composite. The inhibition rate of nano HAP on bone cancer cells, U2-OS cells, was examined. And the effects of nano HAP on mechanical strength of the synthesized composite were also studied.

Correspondence to: Qiang Fu; e-mail: fuharry@hotmail.com
Contract grant sponsor: Chinese Nature Science Foundation; contract grant number: 50272041
Contract grant sponsor: Nanotechnology Special Foundation of Shanghai Science and Technology Committee; contract grant number: 0144NM064

MATERIALS AND METHODS

Materials

Glass composition was designed on consideration of a self-setting $Ca_3(PO_4)_2$ and $CaSiO_3$ crystals, which possessed a high mechanical strength. With respect to the preparation

TABLE I
Ion Concentration (m*M*) in SBF and in Human Blood Plasma[a]

Ion	Na^+	K^+	Mg^{2+}	Ca^{2+}	Cl^-	HCO_3^-	HPO_4^{2-}	SO_4^{2-}
SBF	142.0	5.0	1.5	2.5	147.8	4.2	1.0	0.5
Human plasma	142.0	5.0	1.5	2.5	103.0	27.0	1.0	0.5

[a]From Filho et al.[10]

process and the properties of the final glass, glass with a nominal composition of CaO 45, SiO_2 35, and P_2O_5 20 by weight ratio was selected. Glass batch was melted in an SiC furnace at 1500°C for 4–6 h. The melt was quenched into glass between stainless plates, and then the glass was crushed and pulverized in an aluminum-ball mill into fine powder (3–5 μm).

Nanoscale HAP crystallite was developed through a wet-chemistry method using $Ca(NO_3)_2$ and $(NH_4)_2HPO_4$. The molar ratio of calcium to phosphate was maintained 1.67. $(NH_4)_2HPO_4$ solution was slowly added to $Ca(NO_3)_2$ solution to produce HAP sol. After aging for 24 h, HAP sol was filtered and washed several times. The sol was dried in an oven for a certain time and then the as-dried HAP was milled. The particles produced were spherical HAP crystallite with the average size of 20–40 nm. Micron HAP, with the average size of 1–4 μm, was purchased from Shanghai Medicine Corporation.

$(NH_4)_2HPO_4$ and $NH_4H_2PO_4$ with analytical reagent grade were dissolved in deionized water at a certain ratio to prepare an ammonium phosphate medium solution with a pH value of 7.4.

Bioactive bone cement was produced by mixing the powder (glass powder and nanoscale HAP crystallite or glass powder and micron HAP) with the ammonium phosphate medium evenly. The specimens were immersed in simulated body fluid (SBF) at 37°C. The SBF solution is the closest to human plasma, as shown in Table I.[7]

Methods

Compressive strength of bone cement, composed of nanoscale HAP or micron HAP and glass powder, was measured using an Instron universal testing machine (Instron 1195, Instron Limited, Buckinghamshire, UK) at a crosshead speed of 0.5 mm/min. Cylindrical specimens (6 mm in diameter, 12 mm in length) of bone cement were measured under wet conditions at room temperature after immersing in SBF at 37°C for 7, 15, and 30 days, respectively. For each time interval, a mean value was obtained from the measurement of eight samples.

The morphology of as-dried HAP crystallite and the microstructure of GBC and glass based nano HAP bone cement (designated as GBNHAPC) were observed using field emission scanning electron microscopy (Hitachi JSM-6700F, Hitachi, Japan). The functional groups in both types of cement was analyzed by XRD (D/max 2550v, Rigaku, Tokyo, Japan) and FTIR (FTS-40 Biorad, Digilab Division, Cambridge, MA).

Cell proliferation

Osteosarcoma U2-OS cells were obtained from Institute of Cell Biology of Chinese Academy of Science (Shanghai, China). U2-OS cells (3000 cell/ml) were cultured in RPMI medium 1640 (Gibco) supplemented with 10% fetal bovine serum (FBS, Gibco), 2 m*M* glutamine, 1 m*M* sodium pruvate, 100 U ml^{-1} of penicillin, 100 μg/mL of streptomycin and 50 μg/mL of ascorbic acid. U2-OS cells were plated into 96-well culture plate, 0.2 mL in each well, maintained at 37°C in a fully humidified atmosphere at 5% CO_2 in air for 24 h. Then the medium in control groups was replaced by fresh medium and medium in the trial groups was replaced by nanoscale HAP suspension and micrometer HAP suspension, respectively. Suspensions (250 μg/mL) were made by mixing nanoscale HAP and micrometer HAP with the RPMI medium 1640, respectively.

Cell proliferation was measured using the MTT (3-[4,5-dimethyl-2-thya- zolyl]-2,5-diphenyl-^{2}H-tetrazolium-bromide, Merck, Schuchardt, Germany) test and was determined at 1, 2, and 3 days. The medium was removed and 0.2 mL MTT solution was added to each well. After incubation at 37°C for 4 h in a fully humidified atmosphere at 5% CO_2 in air, the untransformed MTT was removed and 0.3 mL of isopropanol was added, and the optical density was measured using ELISA (enzyme-linked immunosorbent assays) reader (EL311SX, AutoReader, Bio-Tek Instruments, Winooski, VT) at a wavelength of 570 nm. A mean value was obtained from the measurement of eight samples.

The inhibition rate of nanoscale HAP or micrometer HAP was assessed by the following formula:

$$\frac{\text{Trial group OD value} - \text{control group OD value}}{\text{Control group OD value}} \times 100\%$$

Three samples for each material or control were randomly processed for scanning electron microscope (SEM): cells grown on the material were fixed in 2.5% glutaraldehyde, in pH 7.4 phosphate buffer 0.01*M* for 1 h, and dehydrated at a graded ethanol series. Then, samples were washed four times in liquid CO_2 and submitted to critical point dehydration in CO_2 atmosphere (80 atm at 33°C). Finally, the samples were mounted on aluminum stubs for SEM analysis, earthed with silver glue, and then metallized with a thin film (25Å) with Au-Pd. The stubs were examined at 20 kV with a current of 60 μA on SEM.

Statistical analysis

Values are expressed as mean ± standard deviation (SD) and were compared using two-way ANOVA. Subsequently,

TABLE II
Inhibition Rate (%) of Nanoscale HAP and Micron HAP on Osteosarcoma U2-OS Cells

Groups	Time/day		
	1	2	3
Micron HAP	37.4 ± 2.5	28.0 ± 1.7	21.0 ± 1.9
Nanoscale HAP	41.2 ± 2.0	56.3 ± 2.9	73.4 ± 3.1

ANOVA at a 0.05 level of significance between Micron HAP and Nannoscale HAP at the same days. At 1 day, the pair between micro HAP and nanoscale HAP was not significant, $p = 0.3529$. At 2 and 3 days, all pairs were significant.

ANOVA at a 0.05 level of significance among 1, 2 and 3 days in each HAP crystal. In both micron HAP and nanoscale HAP, all pairs were significant. Simple regression, inhibition rate vs. culture time: in micron HAP, $Y = 44.752 - 8.052X$, $r = -0.995$, $p < 0.0001$; in nanoscale HAP, $Y = 25.049 + 15.981X$, $r = 0.999$, $p < 0.0001$.

possible differences were investigated in a post hoc test using Fisher's protected least significant difference (Fisher's PLSD, Stat View, Version 4.02, Apple Corporation). Differences at $p < 0.05$ were considered to be statistically significant.

RESULTS

Effect of nanoscale HAP on osteosarcoma U2-OS cells

The effects of nanoscale HAP and micron HAP on osteosarcoma U2-OS cells proliferation was investigated and the results were shown in Table II.

It could be seen from Table II that nanoscale HAP has a greater effect on U2-OS cell proliferation than micron HAP. The inhibition rate of nanoscale HAP grows with the time and reaches 73.4 ± 3.1% after 3 days.

In order to study the morphology changes of U2-OS cells, three samples were observed using SEM, shown in Figure 1.

It was seen that in the control group [Fig. 1(a)] the cells grew well and all the cells possessed a shuttle-like shape. In Figure 1(b), although they grew quite well, some particles appeared in the cells. In Figure 1(c), the morphology of the cells changed greatly compared with that of (a) and (b). The sizes of the cells differed from one another and the shape changed from a shuttle-like shape to a spherical or elliptical shape. Most of the cells showed the trend of being morphologically altered by nanoscale HAP particles.

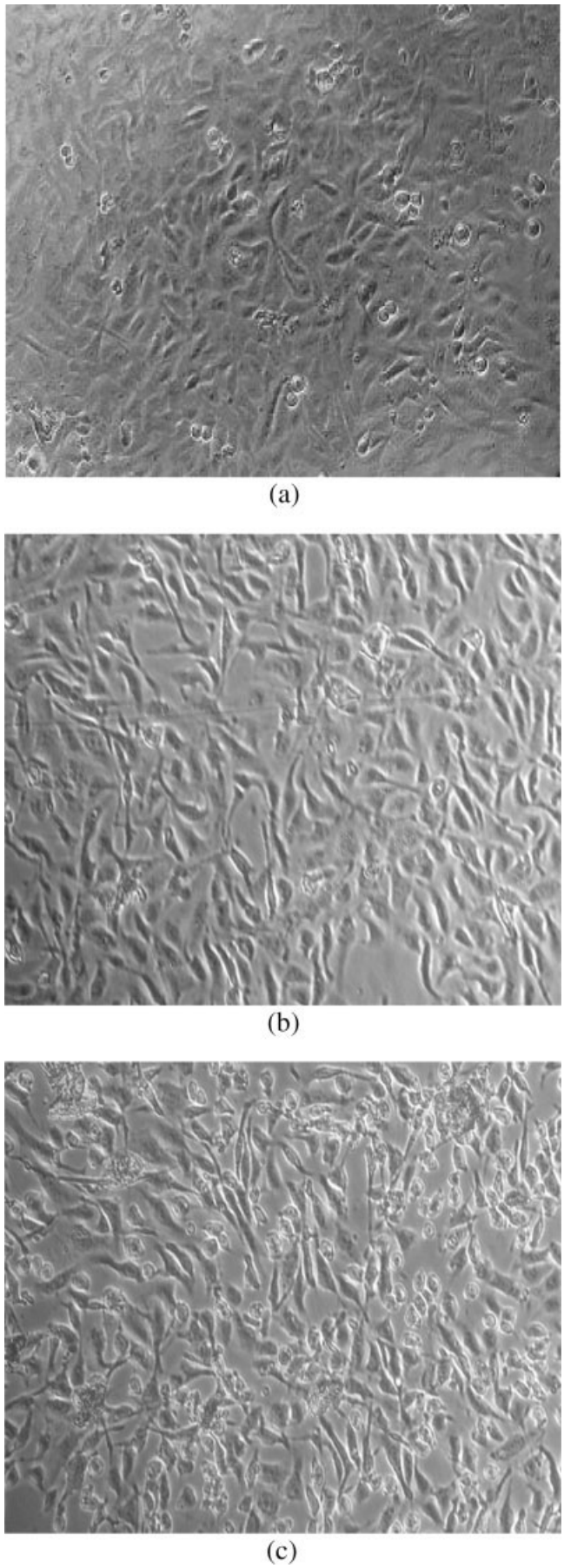

Figure 1. Morphology of U2-OS cells in different culture medium. (a) Pure culture medium; (b) culture medium with micron HAP; (c) culture medium with nanoscale HAP.

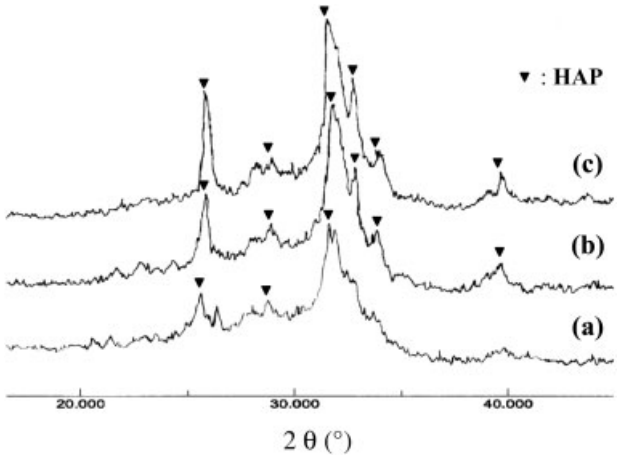

Figure 2. XRD spectra of GBC after different immersion time.

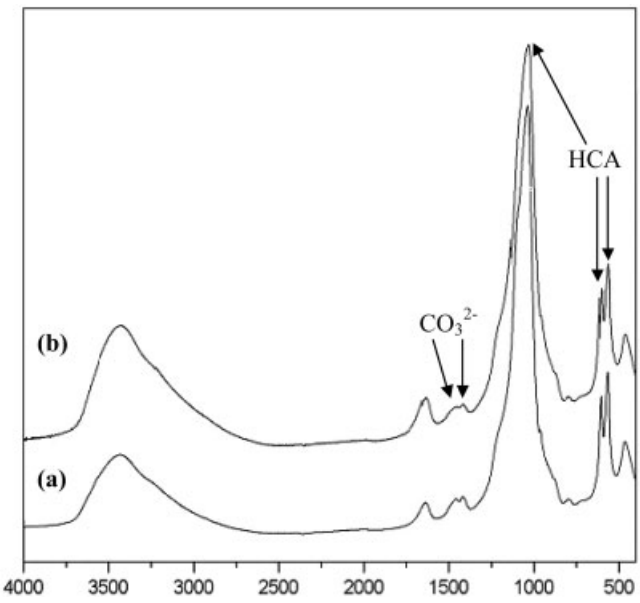

Figure 4. FTIR spectra of bone cement after 7 days immersion time.

Effects of nano HAP on the properties of GBC

Crystal phase analysis

Samples of different immersion time in SBF were analyzed using XRD. Figures 2 and 3 show XRD spectra of GBC and GBNHAPC, respectively, at different immersion times.

Both figures indicate that with the increasing of immersion time, XRD peaks of the two cements became sharper and narrower. They also show that a certain amount of primary HAP crystal has occurred after immersing for 7 days. With the proceeding of immersion, the crystallinity of HAP generated by GBNHAPC and GBC was improved and also the size of primary HAP grew larger. Comparing Figure 2 with Figure 3, it was clear that XRD peaks of GBNHAPC were sharper than that of GBC and the intensity was also higher. Because the addition of apatite seeds could promote the formation of deposited apatite once they provided nucleation sites for HAP crystal growth,[8,9] an improved crystallinity of HAP could be achieved, which could be seen from the sharper XRD peaks of GBNHAPC (see Fig. 3) than that of GBC (see Fig. 2).

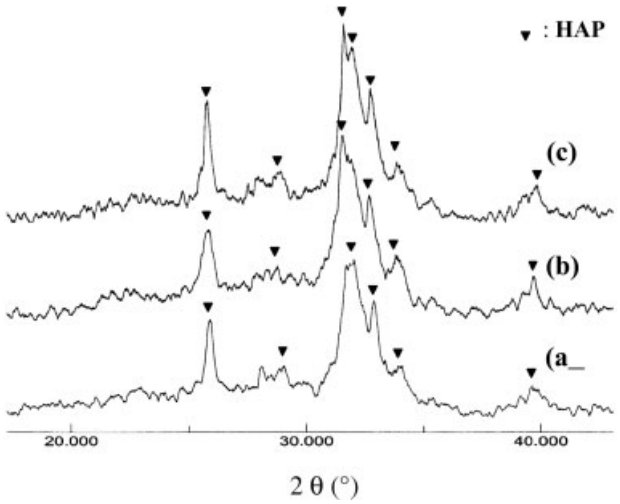

Figure 3. XRD spectra of GBNHAPC after different immersion time.

Functional groups in GBC and GBNHAPC were analyzed using FTIR, shown in Figure 4. It can be seen from Figure 4 that functional groups in both cements are the same. Peaks of 1420 and 1450 cm^{-1} corresponded to the splitting and entrance of CO_3^{2-} groups into HA crystal. Peaks of 560 and 602 cm^{-1}, corresponding to the bending vibration of crystal P—O bond, and 1080 cm^{-1}, corresponding to the stretching vibration of P═O bond, indicate the formation of hydroxy-carbonate apatite (HCA) in GBC.[10,11] The peak of 464 cm^{-1}, corresponding to the transformation vibration of O—Si—O, indicates the appearance of the SiO_2-rich layer in GBC.

Compressive strength

The compressive strength of GBC, GBNHAPC, or glass based micron HAP bone cement (designated as GBMC) after different immersion time in SBF was measured. The results are shown in Table III and Figure 5.

It could be seen that the compressive strength of three bone cement- GBC, GBNHAPC, and GBMC—increased with a longer immersion time. Figure 5 also shows that the bone cement with nanoscale HAP

TABLE III
Compressive Strength of Bone Cement after Different Immersion Time

	Immersion days				
Cements	0	1	7	15	30
GBC	25.3 ± 1.3	45.2 ± 1.8	65.5 ± 2.2	75.4 ± 2.0	80.1 ± 3.0
GBNHAPC	27.1 ± 1.5	50.1 ± 2.0	72.0 ± 2.6	82.4 ± 3.2	92.6 ± 3.8
GBMC	20.0 ± 1.2	35.7 ± 1.5	56.5 ± 2.0	62.3 ± 2.7	65.4 ± 2.5

ANOVA at a 0.05 level of significance among GBC, GBNHAP and GBMC at the same days. At 0 day, the pair between GBC and GBNHAPC was not significantly different, $p = 0.8752$; and neither was the pair between GBC and GBNHAPC at 1 day, $p = 0.2167$. The others pairs at the same days were significantly different. ANOVA at a 0.05 level of significance among 0, 1, 7, 15 and 30 days in each cement. In GBC, all pairs except 15 days vs. 30 days ($p = 0.1359$) were significant. In GBNHAPC, all pairs were significant. In GBMC, all pairs except 15 days vs. 30 days ($p = 0.0874$) were significant. Simple regression, compressive strength vs. immersion days: in GBC, $Y = 35.041 + 1.974X$, $r = 0.837$, $p < 0.0001$; in GBNHAPC, $Y = 37.853+2.334X$, $r = 0.850$, $p < 0.0001$; in GBMC, $Y = 28.831 + 1.577X$, $r = 0.820$, $p < 0.0001$.

reached the highest compressive strength, with GBMC the lowest.

Microstructure

Nanoscale HAP synthesized in the experiment was observed under SEM. Figure 6 shows that the as-dried HAP bore a spherical shape, with the sized ranged from 20 to 40 nm.

The microstructure of GBC and GBNHAPC samples immersed in SBF for 7, 15, and 30 days, respectively, were observed under SEM.

Figures 7(a) and 8(a) show that after immersing in SBF for 7 days, spherical HAP crystals appeared in both GBC and GBNHAPC, and that there were more HAP crystals in GBNHAPC than in GBC. Many nano spherical HAP crystals added were scattered on the glass powder surfaces in GBNHAPC, whereas the HAP crystals appeared at the interfaces of glass powder in GBC. This implies that after 7 days nano HAP could remain its morphology, spherical shape at 20–40 nm, in GBNHAPC.

The obvious differences in microstructure of GBC and GBNHAPC after 15 days were observed in Figures 7(b) and 8(b). The amount of HAP formed was still quite little bearing a spherical shape in GBC, whereas more crystals were observed and some cylinder crystals appeared in GBNHAPC. Considering the components of the both cements, the cylinder crystals were attributed to the addition of nano HAP crystallite. From the comparison of the two pictures, it is known that nano HAP crystallite changed from a spherical shape to a cylinder shape and the length of these cylinders reached about 100–200 nm, with the crystal granularity end size of 20–40 nm.

After 30 days, more cylinder crystals were observed in GBNHAPC [see Fig. 8(c)]. These cylinder HAP crystals filled into the interspaces between glass powder interfaces and formed a chemical bond with glass powder, resulting in the notable increase of the mechanical strength of the cement.

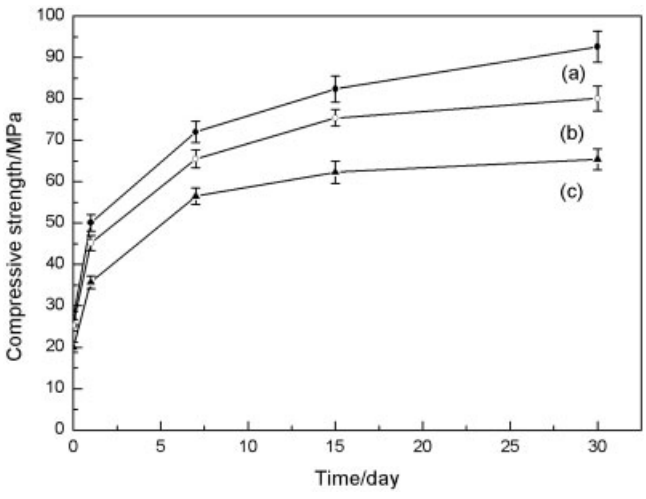

Figure 5. Compressive strength of bone cement after different immersion time. (a) GBC; (b) GBNHAPC; (c) GBMC.

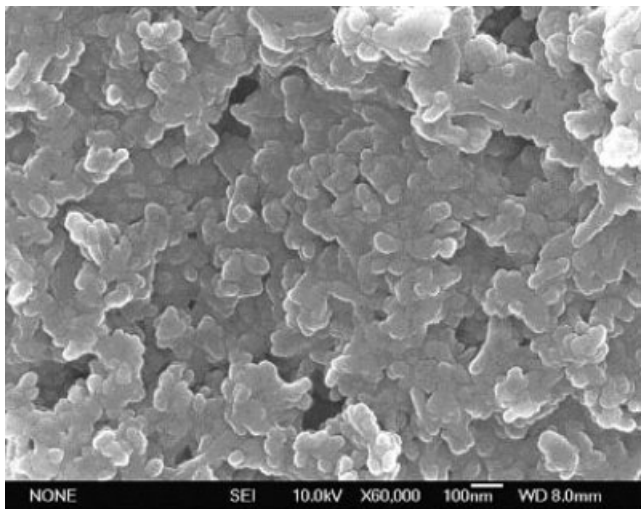

Figure 6. SEM pictures of as-dried nanoscale HAP crystallite.

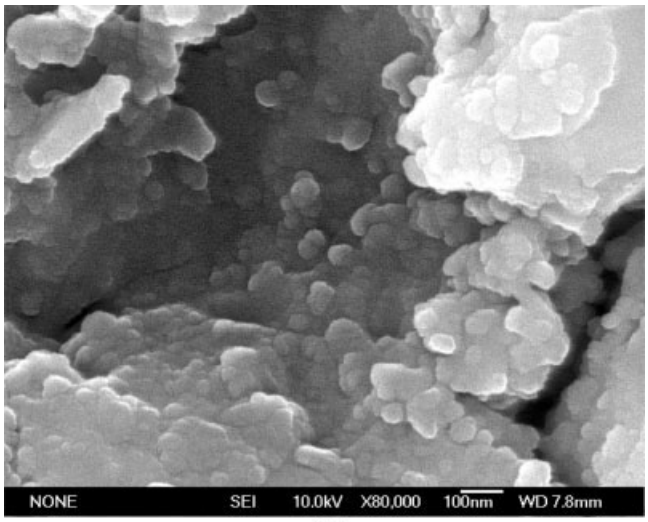

(a)

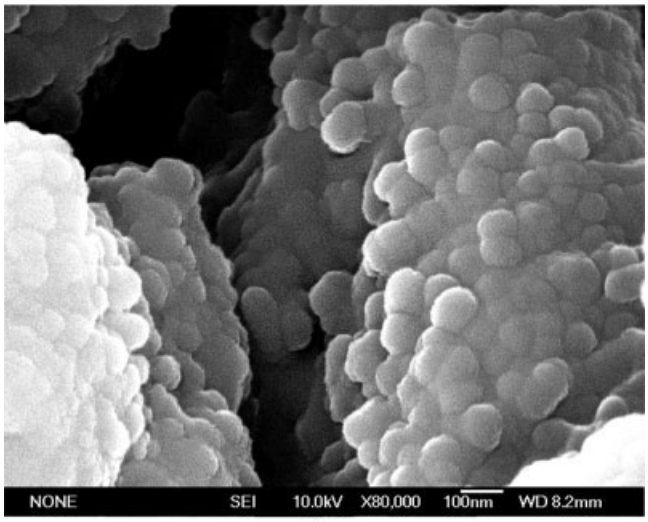

(b)

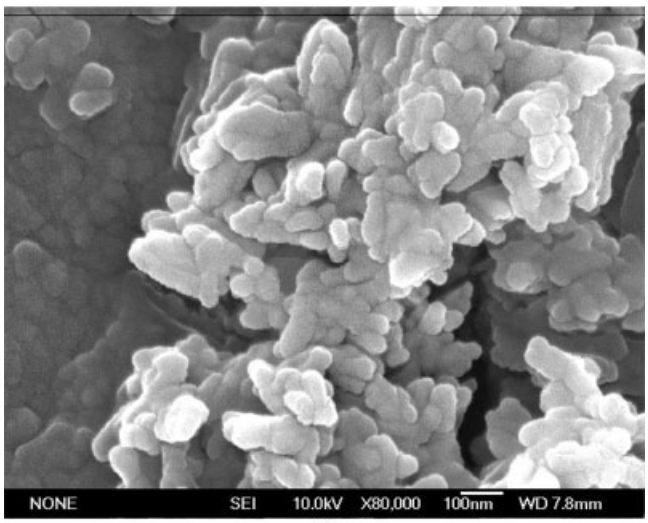

(c)

Figure 7. SEM pictures of GBC samples obtained after different immersion time.

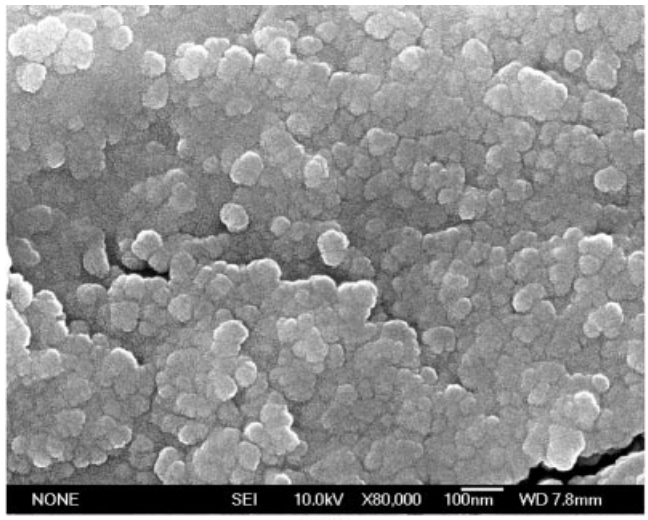

(a)

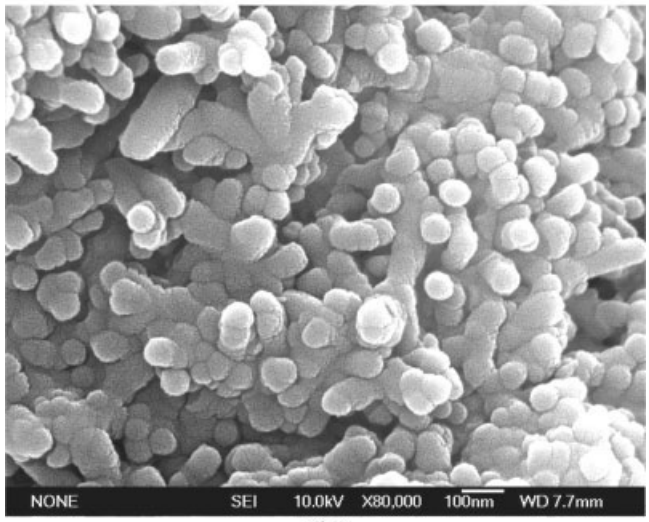

(b)

(c)

Figure 8. SEM pictures of GBNHAPC samples obtained after different immersion time.

It could be concluded that a longer immersion time in SBF had little effect on the morphology of nanoscale HAP and the granularity end of it still ranged from 20 to 40 nm.

DISCUSSION

A desirable biomaterial for repairing bone defects after tumorotomy operation should be able to inhibit the cancer cell growth around the defects, as well as bearing load from the body. Great efforts have been concentrated on the drug delivery system using CPC or GBC as a medium.[12,13] This system, by carrying antibiotic drugs in cement, can inhibit certain kind of cancer cells growth. However, because of the disturbance of the drugs on the hydration reactions of the cement, the mechanical strength, crystal phase, and microstructure are greatly affected. Especially, the mechanical strength decreased greatly. In this study, we examined the effects of nanoscale HAP and micron HAP on the osteosarcoma U2-OS cells proliferation, compared the mechanical strength of cement containing nanoscale HAP and micron HAP, and studied the crystal phase and microstructure of the bone cement containing nanoscale HAP. Our results show that nanoscale HAP was more effective for the inhibition of a certain kind of bone cancer cells, osteosarcoma U2-OS cells, and that the mechanical strength of GBNHAPC was also much greater than that of GBC or bone cement containing micron HAP.

Previous work has shown that nano HAP could inhibit the proliferation of such cancer cells as liver, paunch, and throat cancer cells.[14,15] However, no results concerning the effects of nanoscaele HAP on bone cancer cells proliferation have been reported. In our work, we choose a regular cancer cell, osteosarcoma U2-OS cell, for our experiments and micron HAP as a control group for nanoscale HAP. Our results reveal that the inhibition rate of nano HAP on osteosarcoma U2-OS cell increased with time, whereas that of micron HAP decreased greatly. As calmodulin (CaM) at the cancer cells surfaces was several times higher than at the normal cells surfaces, the proliferation of cancer cells tended to be affected by calcium ion concentration around them. Therefore, calcium ion released from nano HAP and micron HAP may result in the more absorption of calcium ion into cancer cells, leading to the lower growth rate of them. Furthermore, nanoscale HAP ranged from 10 to 50 nm, which has a higher solubility, surface energy, ion exchange capability and polarization, differs greatly from micron HAP in chemical and physical properties. This makes it easier for nanoscale HAP to react with the cancer cells surfaces or even to enter the cancer cells. Therefore, the cancer cell growth was greatly inhibited by nanoscale HAP.

Our work also shows that GBNHAPC had the highest mechanical strength in the three bone cements (GBC, GBNHAPC, and bone cement containing micron HAP) and that the hydration reaction of the cement was not affected by nano HAP, which could be inferred from the similarity of the crystal phase, shown in Figures 2, 3, and 4, respectively. The SEM picture of the microstructure of GBNHAPC indicates that the morphology of the added nanoscale HAP in bone cement did not change greatly, which guaranteed the inhibition ability of it on cancer cells, and that the nano HAP added could also lead to a notable increase of mechanical strength.

CONCLUSION

In summary, the effect of nanoscale HAP on cancer cells proliferation and on glass bone cement properties were examined. Our study shows that nanoscale HAP could inhibit the U2-OS cell proliferation and enhance the mechanical strength of glass bone cement, with little effect on the hydration reaction of the cement.

The authors express thanks to the Chinese Nature Science Foundation (NSF grant number 50272041) and the Nanotechnology Special Foundation of Shanghai Science and Technology Committee (grant number 0144NM064) for their financial support.

References

1. Campanacci M, Baldini N, Boriani S, Sudanese A. Giant cell tumor of bone. J Bone Joint Surg (Am) 1987;69(1):106–114.
2. Bini SA, Gill K, Johnson JO. Giant cell tumor of bone: curettage and cement reconstruction. Clin Orthop 1995;321:245–252.
3. Malony WJ, Jasty M, Rosemberg A, Harris WH. Bone lysis in well-fixed cemented femoral components. J Bone Joint Surg 1990;72-B:966–970.
4. Hamanishi C, Kitamoto K, Tanaka S, Otsuka M, Doi Y, Kitahashi T. A self-setting TTCP-DCPP apatite cement for release of vanconycin. J Biomed Mater Res (Appl Biomater) 1996;33: 139–143.
5. Otsuka M, Matsuda Y, Suwa Y, Fox JL, Higuchi WL. A novel skeletal drug delivery system using a self-setting calcium phosphate cement. Mixing solution volume on the drug release rate of heterogeneous asprin-loaded cement. J Pharm Sci 1994; 83(2):259–263.
6. Tamura J, Kawanabe K, Kobayashi M, Nakamura T, Kokubo T, Yoshihara S, Shibuya T. Mechanical and biological properties of two types of bioactive bone cements consisting Mgo-CaO-SiO_2-P_2O_5-CaF_2 glass and glass-ceramic powder. J Biomed Mater Res 1996;30(1):85–94.
7. Shinzato S, Nakamura T, Tamura J, Kokubo T, Kitamura Y. Bioactive bone cement: effects of phosphoric ester monomer on

mechanical properties and osteoconductvity. J Biomed Mater Res 2001;56:571–577.
8. Liu CS, Shen W. Effect of crystal seeding on the hydration of calcium phosphate cement. J Mater Sci Mater Med 1997;8:803–807.
9. Yang, Q Troczynski T, Liu DM. Influence of apatite seeds on the synthesis of calcium phosphate cement. Biomaterials 2002; 23:2751–2760.
10. Filho O, Torre L, Hench L. Effect of crystallization on apatite-layer formation of bioactive glass 45s5. J Biomed Mater Res 1996;30:509–514.
11. Kokubo T, Kushitani H, Sakka S, Kitsugi T, Yamamuro T. Solutions able to reproduce in vivo surface-structure changes in bioactive glass-ceramic AW. J Biomed Mater Res 1990;24: 721–734.
12. Bohner M, Lemaître J, Landuyt P Van, Zambelli PY, Merkle HP, Gander B. Gentamicin-loaded hydraulic calcium phosphate bone cement as antibiotic delivery system. J Pharm Sci 1997;86:565–572.
13. Otsuka M, Sawada M, Matsuda Y, Nakamura T, Kokubo T. Antibiotic delivery system using bioactive bone cement consisting of Bis-GMA/TEGDMA resin and bioactive glass ceramics. Biomaterials 1997;18:1559–1564.
14. Zhang S, Li S, Chen F. Studies on effects of apatite ultrafine powder on cancer cells. J Wuhan University of Technology 1996;18 (1):5–8.
15. Aoki H, Ogaki M, Kano S. Effects of Adriacin-absorbing hydroxyapatite-sol on Ca-9 cell growth. Rep Inst Med Dent Eng 1993;27(1):39–44.